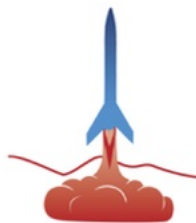
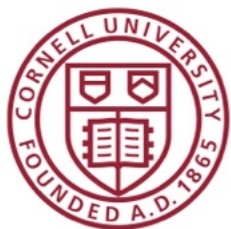


Spring 2025 Technical Report

Thomas Rimer [tr382]
Cornell Rocketry Team
Payload Analysis
Recovery and Payload

Cornell University
Sibley School of Mechanical and Aerospace Engineering
124 Hoy Road
Ithaca, NY 14850



SPACEPORT AMERICA®
CUP

1 System Overview



Figure 1: Fully Assembled Payload

Cornell Rocketry’s payload for the 2025 IREC Competition is a first-of-its-kind dust analysis device that captures and characterizes particulate in the lower atmosphere through a hole in the rocket’s nosecone. This analysis unlocks a new form of airborne particulate monitoring impossible through existing in-situ and remote monitoring technologies.

1.1 Motivation

The lower atmosphere (less than 60,000 feet) is full of contaminants—like heavy metals, chemical aerosols, and dust—which contribute to both climate change and human health problems. Despite the importance of quantifying these airborne contaminants, the two predominant measurement techniques used for tracking both have significant shortcomings. Satellites offer large coverage and continuous monitoring at the cost of low spatial resolution and data “collimation” (readings are lump-sums of contaminants above a given square region; no altitude information is available). Balloons (and occasionally airplanes), give hyper local results at the cost of frequency and often carry less sophisticated equipment.

Rockets provide a unique platform for atmospheric measurements; due to their near-perfect vertical and instant flight, rockets can collect information on contaminant altitude distribution in a way not easily achievable with alternative platforms.

Due to the difficulty of measuring certain kinds of contaminants (like airborne heavy metals), dust was selected as our target contaminant due to its relatively large size, prevalence in the desert (as we saw this year), and ease of detection.

1.2 Subsystems Outline

The payload leverages several subsystems in series to perform the analysis.

1.2.1 Tip

Machined aluminum tip in the nose cone allowing dust to enter while minimizing the drag penalty of an opening on the rocket.

1.2.2 Transfer Tube

Internal ducting to smoothly redirect air from the tip to the top of the payload.

1.2.3 Superstructure

A versatile frame that allows for easy assembly and disassembly of the payload, while remaining flexible enough for inevitable design changes.

1.2.4 Venturi Scrubber

Atomized water is introduced into the air stream prior to a converging throat, encouraging particle capture in the micron-sized water droplets.

1.2.5 Collection Chamber

Colloidal dust is captured in a spherical chamber with a servo-actuated valve for subsequent processing.

1.2.6 Coulter Counter

An aperture-tube based coulter counter captures colloidal dust and analyzes it with custom SRAD electronics.

2 Images of Design

2.1 System Photos



Figure 2: Fully Assembled Payload

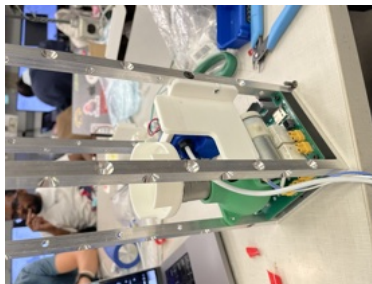


Figure 3: Analysis Section View 1

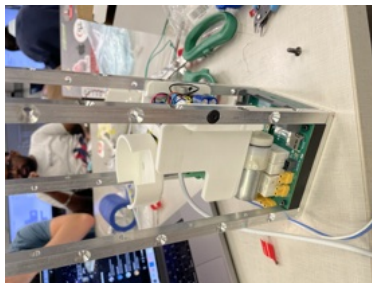


Figure 4: Analysis Section View 2



Figure 5: **Power PCB in Superstructure View 1**

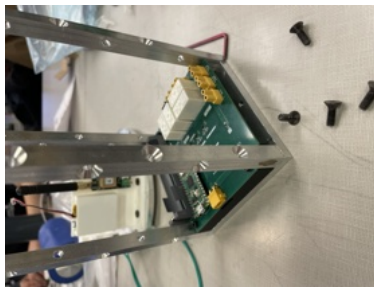


Figure 6: **Power PCB in Superstructure View 2**



Figure 7: **Power PCB Top**



Figure 8: **Power PCB Bottom**

2.2 CAD Assembly

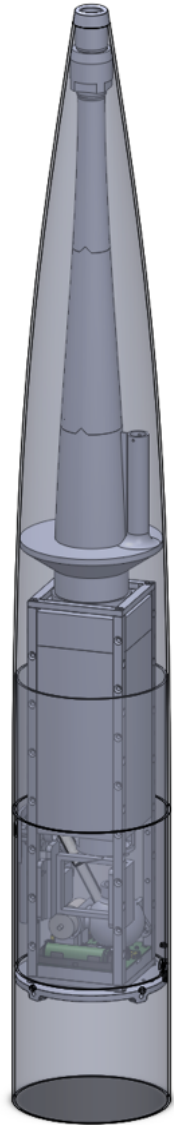


Figure 9: Payload Complete Assembly

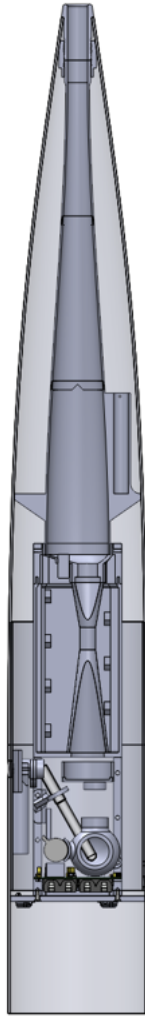


Figure 10: **Payload Complete Assembly Cross Section**

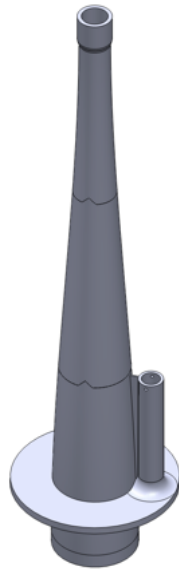


Figure 11: **Transfer Tube View 1**

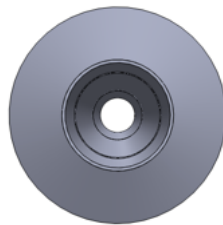


Figure 12: **Transfer Tube View View 2**



Figure 13: **Transfer Tube View View 3**

2.3 CAD Parts

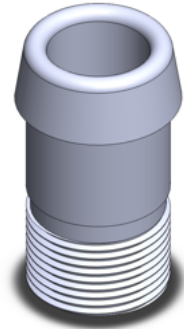


Figure 14: **Tip Body**



Figure 15: **Transfer Tube Upper Section**



Figure 16: **Transfer Tube Middle Section**

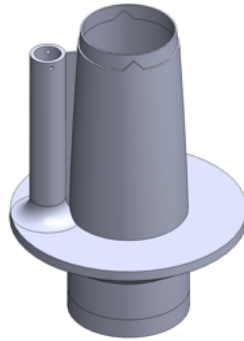


Figure 17: **Transfer Tube Lower Section**

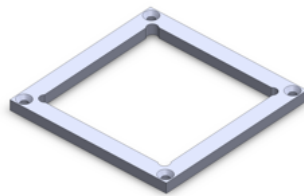


Figure 18: **Superstructure Top Plate**



Figure 19: **Superstructure Vertical Post**

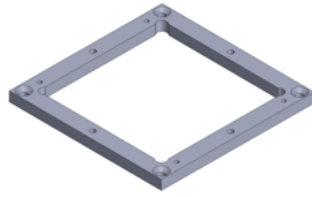


Figure 20: **Superstructure Bottom Plate**

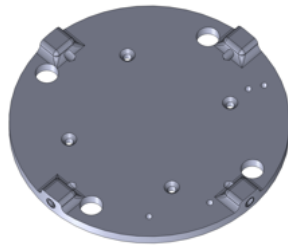


Figure 21: **Superstructure Bulkhead (Top)**

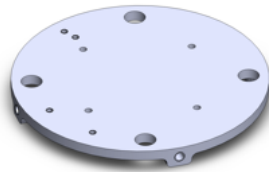


Figure 22: **Superstructure Bulkhead (Bottom)**

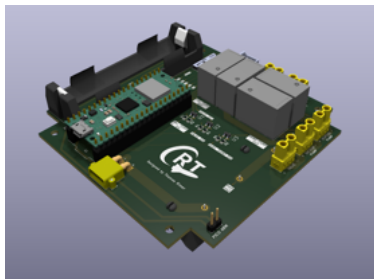


Figure 23: **Payload Power Board View 1**

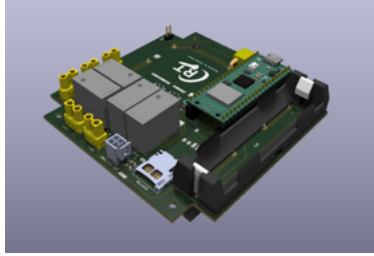


Figure 24: Payload Power Board View 2

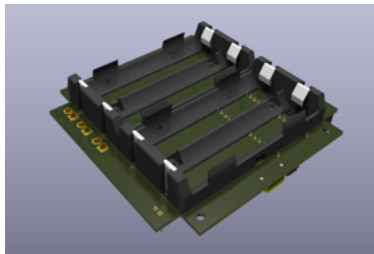


Figure 25: Payload Power Board Underside

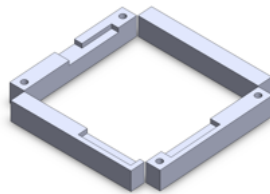


Figure 26: Payload Power Board Risers

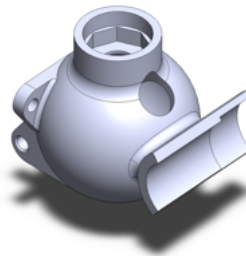


Figure 27: Analysis Tank View 1



Figure 28: **Analysis Tank View 2**

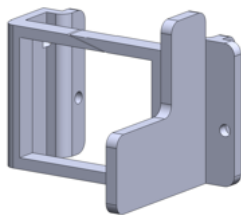


Figure 29: **Ball Valve Mount View 1**

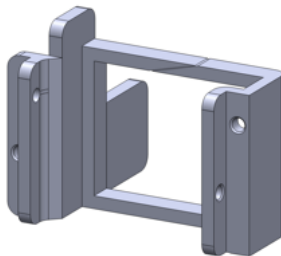


Figure 30: **Ball Valve Mount View 2**

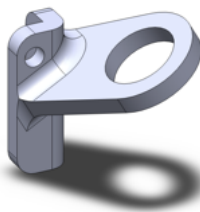


Figure 31: **Aperture Tube Mount View 1**



Figure 32: Aperture Tube Mount View 2

3 System Function

3.1 Relation to Other Systems

By requirement of the competition, the payload must be an entirely self-contained system with no effect on the flight of the rocket (other than its inherent weight) or other systems. As such, the relationship to other systems is limited to the mounting and integration of payload in the nose cone and upper air-frame section.

4 Requirements

4.1 Exogenous Requirements

Exogenous requirements are constraints set by other systems that any payload design must work around or take into account. Any and every approach to designing payload is subject to the same exogenous requirements.

4.1.1 Cubesat Formfactor

The Spaceport America Cup awards extra points for teams' payloads to fit a standard 1U, 2U, 3U, or 4U cubesat formfactor. Due to the number of mechanisms inside payload, a 4U (10cm x 10cm x 40cm) package was chosen at the beginning of the project and all designs were modeled off it.

4.1.2 Airframe and Nosecone

Due to the inherent nature of dust sampling, any design for payload needs access to the air flowing around the rocket. This could in principle be achieved through any port to outside air, but risk of contamination from air flow traveling over other sections of the airframe limits the inlet to the tip or area immediately surrounding the tip. Therefore, the payload must necessarily have some section in the payload.

4.1.3 Drag

Due to initial concerns regarding the rocket motor's impulse and peak thrust, the drag induced by sampling the air must be reduced as much as practical. Furthermore, drag should ideally be symmetric to avoid inadvertently pitching the rocket one way or another.

4.1.4 Mass

The IREC 2025 rules mandate the payload must be no less than 4.4lbs [1].

Due to concerns regarding underpowered propulsion, payload was to be minimized as much as practically possible. This was further exacerbated by the distance of Payload from the rocket's center of mass, which meant small increases in payload mass has large impacts on the stability and performance of the rocket.

4.1.5 Temperature

As will all systems inside the rocket, launch conditions are extreme. During winter launches, temperatures regularly dip below 0°F. During summer (competition) launches, temperature inside the rocket can exceed 150°F. Any design must be capable of operating as intended within this range.

4.1.6 Miscellaneous COTS Modules

A Featherweight [2] GPS module was to be included in the nose cone and therefore sufficient room must be available for its mounting.

4.2 Endogenous Requirements

Endogenous requirements are constraints specific to a certain implementation of payload. Any and every approach to designing BLiMS has a unique set of endogenous requirements which determine the final design.

4.2.1 COTS Aperture Tube

Due to the difficulty of manufacturing 20m features with the machining resources available in the Cornell shop, COTS aperture tubes (orifices with precisely drilled holes on the order of 10-100 m) had to be relied on for the payload coulter counter. Aperture tubes are typically several inches long and are very delicate; the specific payload implementation for payload therefore must design around safely mounting the aperture tube inside the payload without risk of damaging it during launch, descent, or landing.

4.2.2 Accommodating of Design Changes

The payload timeline was significantly delayed due to other concurrent RP projects, therefore many subsystems of payload had to be done in parallel. To ensure system designers had maximum flexibility while still ensuring rapid execution, all subsystems of payload

were designed to be easily modified and accommodating of large and medium design changes down the line.

4.2.3 Rapidly Manufacturable

Spurred by the same delays which compelled systems to be accommodating of design changes, the payload also needed to be rapidly manufacturable to have a chance of finishing completion prior to competition. This involves minimizing number and complexity of machined parts, relying on 3D printing, and reducing overall system complexity through COTS components and simplified designs.

4.2.4 Sustained Cleanliness

The purpose of payload is to measure atmospheric dust. Any contamination from dust lodged inside the payload prior to launch or accumulated dust on the outside of the rocket making its way in not only invalidates the findings, but risks damaging the aperture tube and associated sensitive onboard instruments.

4.3 Design

4.3.1 Design Overview

Payload is comprised of several subsystems as previously mentioned in the subsystems outline above. Below is a description of the performance of the system as a whole.

During the ascent stage of the launch, dust-laden atmospheric air colliding with the front of the rocket is collected through a 0.9" hole in the tip of the nose cone. This air is passed through a 2 ft long 3D printed "transfer tube" from the tip of the nose cone to the top of payload. This tube smoothly expands in cross sectional area from the tip to the top of the payload, ensuring minimal dust dropout on the way to the payload.

At the top of payload is a nozzle which creates a mist of atomized water which is injected into the high speed air stream. The water is pressurized by a pump within payload which is housed in the water tank that holds the 1L of water required for launch.

The dusty air and water droplet mixture travels through a converging section of pipe known as a "venturi scrubber" which forces high speed dust in the air to collide with water droplets which subsequently capture it. After construction, the venturi scrubber expands, once again slowing down the air and allowing it to exit out of two ports on the left and right side of the rocket.

Water droplets contained the captured dust have significant inertia, causing them to collide with the bottom of the venturi scrubber and accumulate at the bottom (rather than following the air stream out the side of the rocket). During ascent stage, a motorized ball valve is opened allowing liquid to flow into a collection chamber. At apogee valve is closed, trapping the collected dust water inside the chamber.

During the descent and after landing, an onboard vacuum pump turns on, pulling liquid through a 20m hole (referred to as the "aperture"). Electrodes on either side of the

aperture record the voltage drop across the aperture, which spikes every time a particle transits the aperture. These spikes are identified and logged by an onboard analysis chip.

4.3.2 Tip Design Considerations

The payload needs air to sample, which is collected through a hole in the nose cone. The larger the hole, the greater the amount of air which can be sampled, and thus the higher change of payload successfully identifying dust. However, a blunt tip will change air flow over the rocket and thus incur some drag penalty, decreasing our ultimate apogee. With anticipated limited propulsion capabilities, understanding the drag penalties incurred with various tip designs was essential.

The objective of the tip shape literature review was therefore to: *Determine a geometry for the nose cone tip that maximizes air intake without significantly impacting the rocket's overall drag.*

To ensure the most reliable results, online reports studying similar blunt-nose geometry were compared to our proposed geometry, with drag coefficients extrapolated through semi-numerical means. This approach was chosen in contrast to hand-based calculations or computer based simulations (like Ansys Fluent) due to the complexity of the calculations and risk of making an indecipherable/unverifiable mistake.

In his 1996 article, the programmer Gary Crowell—one of the creators of the unfindable "VCP" aerodynamics software—provided background into basic nose cone geometries [?]. The document is just useful content, and was never intended to be published in a peer reviewed and/or scientific journal. The beginning of the document summarizes the equations describing the most common nose cone geometries, including the Haack series equations of which Von Karman (when $C=0$) is a specific case. Further sections repeat the findings mentioned above almost word for word. Below is the most relevant excerpt from the document:

"Below Mach .8, the nose pressure drag is essentially zero for all shapes. The major significant factor is friction drag, which is largely dependent upon the wetted area, the surface smoothness of that area, and the presence of any discontinuities in the shape. In strictly subsonic model rockets, a short, blunt, smooth elliptical shape is usually best. In the transonic region and beyond, where the pressure drag increases dramatically, the effect of nose shape on drag becomes highly significant. The factors influencing the pressure drag are the general shape of the nosecone, its fineness ratio, and its bluntness ratio."

Further in the article, the author explains: "Fortunately, there is little or no drag increase for slight blunting of a sharp nose shape. In fact, for constant overall lengths, there is a decrease in drag for bluntness ratios of up to 0.2, with an optimum at about 0.15. A flat truncation of a nose tip is known as a Meplat diameter, and the drag reduction effect of a Meplat truncation is shown in the diagram below."

The author backs up this claim with the following graph:

Fig-4 Me plat truncation and Drag

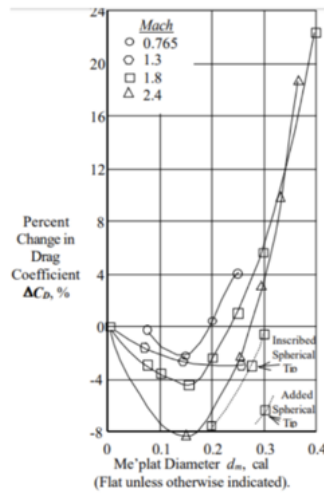


Figure 33: Crowell Drag Graph

There, the payload hole in the end of the nosecone is assumed to behave like a me plat truncation (this is worst case scenario for drag). From the figure above, a me plat diameter caliber of 0.2 is the maximum without a drag penalty. For a 6" air frame, a 0.2 meplat truncation corresponds to a 6"×0.2 = 1.2" blunt tip without penalty, with an optimal diameter of 6"×0.15 = 0.9". The 6:1 Von Karman purchased off the shelf for the rocket has an opening of 1.25" so any hole size must be less than 1.25" to allow for tube liner material and mounting (and avoid cutting the nose cone tip). For round numbers, the tip hole was chosen to be 0.9" allowing sufficient clearance for the aluminum side walls.

To summarize, the nose cone tip was determined to have a 0.9" hole by looking at existing nose cone literature. Surprisingly, the truncation is not expected to impact the drag, and may even slightly reduce drag.

4.3.3 Dust Collection Technique

Significant effort was invested into determining the appropriate dust collection scheme. Initially, filters were chosen for their perceived simplicity of their design and operating principles. However, further investigation demonstrated that filters were not well suited for collection of ultra-fine particulate, with the intention of re-suspending it in solution. Therefore, "wet scrubbers" were instead evaluated.

An initial design for a venturi wet throat scrubber was proposed based on the synthesis of several papers [4] [5]. This design included a tank integrated into the lining of the venturi throat, and served as a starting point for other members to design the final scrubber. Below are photos of the initial wet throat design.

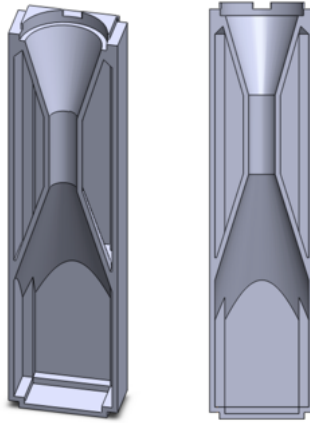


Figure 34: Renderings of Initial Wet Throat Design

4.3.4 Superstructure

The superstructure had two primary goals. Firstly, it needed to serve as a backbone for the entire payload, with sufficient structural integrity to support any and all systems within payload during launch, descent, deployment, and landing. Furthermore, it needed to be highly adaptable to different designs; this meant keeping it as low-profile as possible, and providing many general-purpose mounting points on which future components could be fixed.

To achieve these goals, 4x 3/8" square 6061 aluminum bars were used as posts, mounted via a tapped hole in their end to top and bottom plates made from 1/4" aluminum. Along the posts, 1/2" holes alternating on different sides of the post provide mounting points at predictable and easily accessible locations.

An aluminum bulkhead with four radial holes was used as the single structural mount between payload and the airframe. Holes in the bottom plate of the payload superstructure allowed the superstructure to be easily mounted and dismounted.

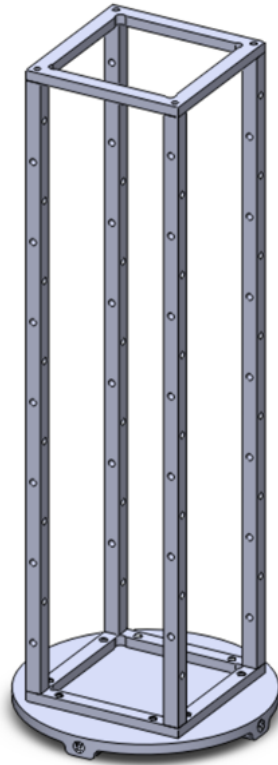


Figure 35: **Payload superstructure and Mounting Bulkhead**

4.3.5 Analysis Section

The analysis section consists of a motorized 1/4" ball valve which regulates the flow of fluid in and out of a spherical, 1.25" diameter 3D printed tank. The aperture tube, 4.5" in length, is mounted in the side of the tank through a waterproof and vibration damping rubber gasket. The tip of the aperture tube is precisely located in the middle of the tank, ensuring its submerged regardless of rocket orientation. A miniature vacuum pump, providing the suction necessary to draw fluid through the aperture tube, is mounted on the tank. On the side of the ball valve is the analysis PCB, which houses the microcontroller and voltage references source for reading from the coulter counter.

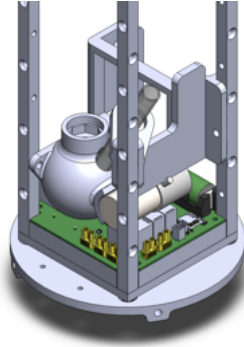


Figure 36: **Analysis Section View 1**

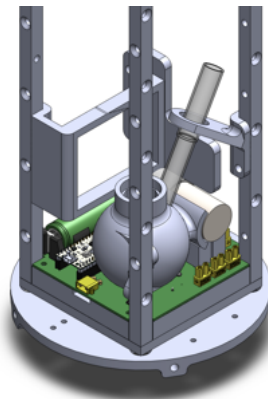


Figure 37: **Analysis Section View 2**

At the very bottom of the analysis section is the payload power PCB, which not only houses the two independent sets of batteries, but also contains the Pico flight controller (responsible for synchronizing the behavior of payload with the rest of the rocket). This board regulates power to the high-current (10+ amp) venturi pump, as well as the vacuum pump and ball valve.

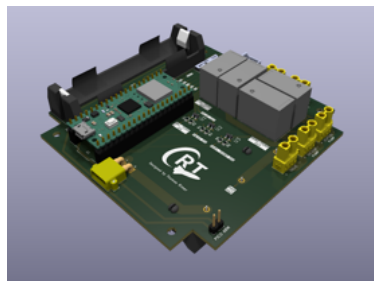


Figure 38: **Payload Power Board View 1**

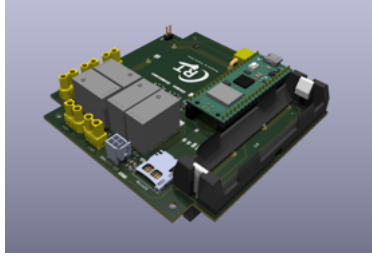


Figure 39: Payload Power Board View 2

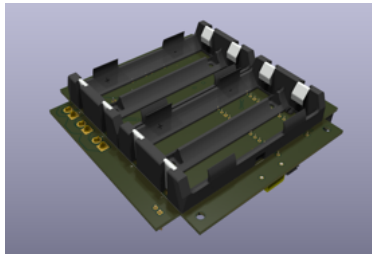


Figure 40: Payload Power Board Underside

4.3.6 Valve Trade Study

Though an SRAD valve was initially considered for its smaller size greater packaging flexibility, a COTS valve was chosen due to its guaranteed performance and faster development time. Twenty nine different ball valves were evaluated, and evaluated in the following "round 1" trade study.

Case	Year	Country	Study Design	Exposure				Outcome	Notes
				Exposure	Exposure	Exposure	Exposure		
1	1998	USA	Case-control
	1999	USA	Case-control
	2000	USA	Case-control
	2001	USA	Case-control
	2002	USA	Case-control
	2003	USA	Case-control
	2004	USA	Case-control
	2005	USA	Case-control
	2006	USA	Case-control
	2007	USA	Case-control
2	2008	USA	Case-control
	2009	USA	Case-control
	2010	USA	Case-control
	2011	USA	Case-control
	2012	USA	Case-control
	2013	USA	Case-control
	2014	USA	Case-control
	2015	USA	Case-control
	2016	USA	Case-control
	2017	USA	Case-control

Figure 41: Payload Power Board Underside

A second round trade study was also performed, imaged below.

Category	Item	Usage		Availability		Performance		Reliability		Notes	Status
		Current	Target	Current	Target	Current	Target	Current	Target		
System	System A	100%	100%	100%	100%	100%	100%	100%	100%	System A is fully operational and meets all requirements.	OK
	System B	95%	100%	90%	100%	95%	100%	90%	100%	System B is mostly operational but has some minor issues.	Warning
Component	Component X	100%	100%	100%	100%	100%	100%	100%	100%	Component X is fully operational and meets all requirements.	OK
	Component Y	90%	100%	85%	100%	90%	100%	85%	100%	Component Y is mostly operational but has some minor issues.	Warning
Module	Module Z	100%	100%	100%	100%	100%	100%	100%	100%	Module Z is fully operational and meets all requirements.	OK
	Module W	95%	100%	90%	100%	95%	100%	90%	100%	Module W is mostly operational but has some minor issues.	Warning

Figure 42: Payload Power Board Underside

The final verdict was a 1 / 4" Steel Ball Valve 9-36V 2-Wire NC Full Port from U.S. Solid.

4.3.7 Coulter Counter Analysis

Before committing to a 20 μm aperture tube, effort was invested into understanding the properties and dynamics of different sized aperture tubes.

Aperture Size The diameter and thickness of the aperture determines many features of the microfluidic system. Therefore, it must first be calculated.

We expect dust up to 10 μm to be present in the atmosphere. The smallest possible aperture size which can accommodate 10 μm particulates is the 20 μm aperture [3]. (Note that the aperture must be at least 25 percent larger than the diameter of the largest particle, so 20 μm can technically accommodate up to 16 μm particles. This agrees with the recommended particle sizes on Beckman Coulter's website. This larger size limit has the added benefit of decreasing the chance of a large particle from clogging the system).

Beckman Coulter does not provide information regarding the thickness of the orifice. We must therefore estimate the orifice volume. Swiss Jewel provides diameters and thicknesses for their whole range of Ring Jewel Bearings, which while not identical to the ruby orifices used in Coulter counters, are close enough to serve as an order-of-magnitude estimate. Using google sheets, a linear fit was created for bearings with 100 μm IDs.

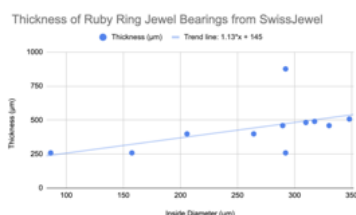


Figure 43: Estimation of Aperture Tube Orifice Thickness

The resulting empirical equation is:

$$\text{thickness (m)} = 1.13 * \text{internal diameter (m)} + 145$$

Therefore, for a 20 μm orifice, we would expect thickness to be $1.13 * 20 + 145 = 167.6$ μm . Therefore, we can conclude that the thickness of the orifice should be somewhere between 100 μm and 200 μm .

Flow Rate Equations to calculate flow rate through an orifice assume thickness of the orifice < diameter of the orifice. However, this is not the case for the Coulter aperture, where thickness is 5x to 10x greater than diameter. Therefore, the Hagen–Poiseuille equation is the most appropriate way to estimate flow rate. The Hagen–Poiseuille assumes incompressible and laminar flow. Note that for the Hagen–Poiseuille to hold, the Reynolds number in the pipe should be less than 48 times the ratio of length to radius of the pipe. The Hagen–Poiseuille equation is:

$$\Delta p = \frac{8\mu L Q}{\pi R^4} = \frac{8\pi\mu L Q}{A^2},$$

where

Δp is the pressure difference between the two ends,

L is the length of pipe,

μ is the dynamic viscosity,

Q is the volumetric flow rate,

R is the pipe radius,

A is the cross-sectional area of pipe.

Let's assume fluid is sucked through the orifice; therefore, the pressure differential has a maximum of 1 atm = 14.69 psi 14 psi. We can therefore rearrange the equation to solve for Q , giving us:

$$Q = \frac{\pi R^4 \Delta p}{8\mu L}$$

Plugging in $R = 10 \cdot 10^{-6}$, $p = 95,000$ Pa, $\mu = 1 \cdot 10^{-3}$ Pa s, and $L = 100 \cdot 10^{-6}$ m (thinner estimate) gives $Q = 3.7 \cdot 10^{-9}$ m³ s⁻¹. Instead plugging in $L = 200 \cdot 10^{-6}$ (thicker estimate) gives $Q = 1.9 \cdot 10^{-9}$ m³ s⁻¹. We can represent these results in the following table:

		Flow Rates			
		m ³ s ⁻¹	mL s ⁻¹	mL min ⁻¹	mL hour ⁻¹
Aperture Thickness	100 μm	3.73E-09	3.73E-03	2.24E-01	1.34E+01
	200 μm	1.87E-09	1.87E-03	1.12E-01	6.72E+00

Figure 44: Table Summarizing Expected Flow Rates Depending of Upper and Lower Limits of Aperture Tube Thickness

For a rough estimate, we should assume we can process 10 mL per hour through the aperture tube assuming we pull a vacuum.

Sampling Rate The electronics must sample frequently enough to catch all voltage spikes. To determine the necessary sampling frequency, we must first calculate the velocities of particles flowing through.

Assume parabolic flow through the aperture. We can use root form of parabola to write an equation for the velocity V as a function of radius from center r

$$V = a(r - R)(r + R)$$

where $R = 10$ m = $10 \cdot 10^{-6}$ m and a is the constant to be determined. We know the flow rate through the tube is equal to the integral of velocity over the cross section of the pipe. In other words

$$Q = \int_{area} V da$$

which can be expanded to

$$\int_{\theta=0}^{2\pi} \int_{r=0}^R a(r-R)(r+R)r dr d\theta$$

Solving for a gives

$$a = -\frac{2Q}{\pi R^4}$$

Plugging in $Q = 2 \cdot 10^{-9} \text{ m}^3 \text{ s}^{-1}$ gives $a = -2.37 \cdot 10^{11}$. Assume particles are flowing through the center of the aperture (traveling at the peak velocity, which is the worst case scenario for the electronics). Therefore, peak velocity is

$$V = -4.775 \cdot 10^{-5} (0 - R)(0 + R)$$

which, after plugging in, gives $V = 23.75 \text{ m/s}$.

We know particles will spend

$$T = \frac{L}{V}$$

seconds in the aperture, where L is length of the aperture and V is velocity. Therefore, given the velocity of 25 m/s given above and $L = 100 \text{ m} = 100 \cdot 10^{-6} \text{ m}$, expected time in the aperture is $T = 4 \cdot 10^{-6}$ seconds.

Let's assume that we need to take at least 10 measurements during the particle's transit. That means we need to sample every $4 \cdot 10^{-7}$ seconds. In frequency, that's 2,500,000 Hz = 2.5 MHz.

Assuming 16 bit sampling depth, that is 40,000,000 bits a second (40 mbps). Over one hour of sampling, that's 17.5 gigabytes of data. This is a brute force approach and is not the most elegant approach. Instead, we would likely want to use a peak detector. That would significantly decrease the required sampling rate (by at least an order of magnitude).

4.3.8 Payload Analysis Board

The layout and component selection of the payload analysis board was handled by other members on the team. However, I did manage the high level system requirements. Below is a diagram showing the overall structure of the payload analysis board.

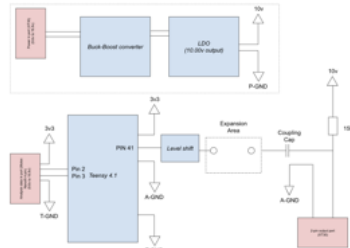


Figure 45: Diagram of the Payload Analysis PCB

4.3.9 Batteries

Onboard the payload power board were two independent sets of batteries; one 12v nominal for powering pumps and other high power electronics, and on 3.3v nominal for powering the microcontrollers. Due to issues with batteries in the past, a major emphasis on payload was ensuring significantly excess power was available for all systems in case of long launch wait times or unexpectedly high draw.

3v3 Nominal Battery A single 18650 Li-Ion cell will provide the 3v3 to the following components:

- Raspberry Pi Pico W
- Teensy 4.1

We expect this setup to provide 14 hours of operation for the microcontrollers. The Li-Ion battery used was the Molicel P28A 18650s from 18650BatteryStore. It has the following characteristics:

Voltage Minimum: 2.5v (=2.5v * 1 battery) Maximum: 4.2v (=5.2v * 1 battery) Nominal: 3.6v (=3.6v * 1 battery)

Current 35 amps continuous (=35 A * 1 battery)

Capacity 2,800 mAh (=2,800 mAh * 1 battery)

Misc Weight: 45 grams (=45 grams * 1 battery) Temperature °C: -40c to +60c Temperature °F: -40f to 140f

The expected current draw from the Raspberry Pi Pico W is 20-30 mA during standby and 80-100 mA during normal operation. During peak loading it may draw up to 150 mA. The Teensy 4.1 has less well-documented information regarding current draw, so it was assumed to be the same as the Pico W.

Therefore, given the Raspberry Pi Pico W pulls 100 mA @ 3.3v, the Teensy 4.1 also pulls 100 mA @ 3.3v. Therefore there is a combined nominal current draw of 200 mA (=100 mA

+ 100 mA). This means that the logic level should be capable of powering the two devices for 14 hours ($=2,800 \text{ mAh} / 200 \text{ mA}$).

12v Nominal Battery Four 18650s wired in series will provide the 12v nominal to the following components: Venturi pump (T7 design) Vacuum pump (Amazon) Valve (must design around two options) Solenoid (McMaster) $\frac{1}{4}$ " motorized ball valve (Amazon)

- Venturi pump
- Vacuum pump
- Valve
- $\frac{1}{4}$ " motorized ball valve

This setup is expected to contain 5.4x times the necessary energy for a single launch. (Note a total X hours operation spec does not make sense because many devices are powered intermittently, so power draw is not constant).

Here are the numbers for a 4x 18650 series battery. All calculations performed using the Molicel P28A 18650s from 18650BatteryStore:

Voltage Minimum: 10v ($=2.5\text{v} * 4 \text{ batteries}$) Maximum: 16.8v ($=4.2\text{v} * 4 \text{ batteries}$)
Nominal: 14.4v ($=3.6\text{v} * 4 \text{ batteries}$)

Current 35 amps continuous (batteries in series do not increase current)

Capacity 2,800 mAh (batteries in series do not increase capacity)

Misc Weight: 180 grams ($=45 \text{ grams} * 4 \text{ batteries}$) Temperature °C: -40c to +60c Temperature °F: -40f to 140f

The expected current draw from each component is as follows: Venturi pump Maximum current (@ 30 psi): 17 A Minimum current (@ 100 psi): 8 A

Vacuum pump Operating current: 0.150 A Standby current: 0 A

Motorized ball valve Maximum current (while actively opening): 0.1 A Open standby current: 0.01 A Closed standby current: 0 A

The ball valve consumes 0.138 mAh when opening ($=100 \text{ mA} * 5 \text{ seconds} / 3600 \text{ seconds}$). The venturi pump consumes 215 mAh ($=17,000 \text{ mA} * 45 \text{ seconds} / 3600 \text{ seconds}$). The vacuum pump will nominally run for 2 hours after landing. Therefore, the vacuum pump consumes 300 mAh ($=150 \text{ mA} * 2$).

Therefore the total energy consumption for launch is 515 mAh ($=0.138 \text{ mAh} + 215 \text{ mAh} + 300 \text{ mAh}$). This means our 4x 18650s provide a 5.4x safety factor ($=2800 \text{ mAh} / 515 \text{ mAh}$).

In practice, the pump will continue running for as long as possible. This means the pump will be able to run for 17 hours ($=(2800 \text{ mAh} - 25 \text{ mAh} - 215 \text{ mAh}) / 150 \text{ mA}$) following the landing.

4.3.10 Mass Makeup

Below is table showing the payload individual component masses

A pie chart was also constructed from the table showing fractional mass of each component.

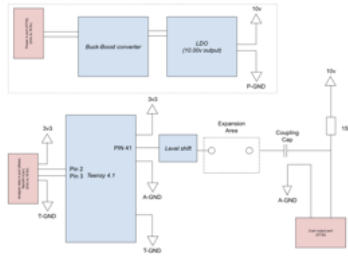


Figure 46: **Diagram of the Payload Analysis PCB**

The upper section (plastic tank and water) represents the heaviest part of payload at over 1/3 of total mass. However, the amount of plastic cannot be significantly reduced—else the tank wall thickness drops below a waterproof threshold—and the volume of water is determined by flow time and other factors.

The payload superstructure represents a little less than 20 percent of the overall mass. This could be reduced further if lighter alloys were used and the top/bottom brackets were thinner but given the importance of a sturdy superstructure this extra weight was deemed necessary.

4.4 Analysis

4.4.1 Particle Size Distribution

Before designing a system to capture dust, the properties of the dust itself must be known. Fortunately, White Sands Missile Range and the surrounding areas are hot spots for dust in the South West and have been studied extensively.

The most relevant resource came from the National Park service, which synthesized the work of several researchers in a webpage outlining dust levels in White Sands National Park [6]. Below is a photograph of the atmospheric dust as seen from a satellite:



Figure 47: **Dust lifted from White Sands National Park from a wind storm, as seen from a satellite**

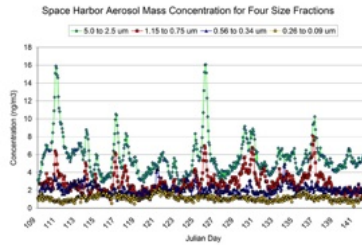


Figure 48: **Ground level dust size distribution at Spaceport America**

From the graph above, the following plots were constructed and a quadratic fit was applied, allowing for a quantitative dust size distribution for further calculations.

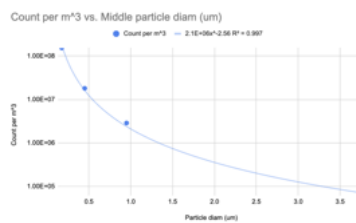


Figure 49: **Number of particle as a function of particle size**

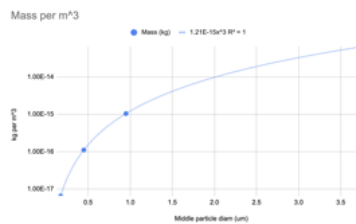


Figure 50: **Mass contribution of different sized particles**

4.4.2 Pump Flow Rate Calculations

To evaluate the feasibility of even using a wet-scrubber style capturing mechanism, flow rates were calculated using air-liquid ratios recommended by the EPA [5].

Background on Air Density It's important to understand the basics of air density, and how it's measured. ACFM (actual cubic feet) refers to the actual cubic feet of air flowing through a system at the current conditions (temperature, pressure, humidity, etc...). SCFM (standard cubic feet per minute) refers to the volume of air flowing through a system if that air were at a standard temperature and pressure (60°F, 14.7 PSI).

Background on Air Temperature Temperature in the atmosphere can be modeled with the following equation

$$T = T_0 - L \left(\frac{h}{1000} \right)$$

where T is temperature, T₀ is temperature at ground, L is linear lapse rate, and h is height above the ground (not to be confused with elevation above sea level). Linear lapse rates are typically 3.5°F per thousand feet, so L = 3.5. This equation holds in the troposphere (up to 35,000 feet). In metric, we have

$$T = T_0 - Lh$$

where L = 0.0065 °K per meter.

At apogee, temperature is 35°F cooler than the ground. If the ground temperature is 100°F, then air temp at apogee is 65°F.

Background on Pressure in the Atmosphere The pressure above the ground is more confusing. It can be modeled with the following equation

$$P(h,h') = P_0 \left(\frac{T_0 - L \cdot h}{T_0} \right)^{\frac{gM}{RL}} \left(\frac{T_{actual,ground} - L \cdot h'}{T_{actual,ground}} \right)^{\frac{gM}{RL}}$$

where h is elevation of ground above sea level in meters (1,219m for White Sands) h' is altitude above ground of air in question (up to 3,048m for our launch) P₀ = 101,325 Pa = standard sea level pressure T₀ is standard temperature = 288.15°K L = 0.0065 = lapse rate in °K per meter from before T_{actual,ground} is the actual air temperature in ° Kelvin at the ground (110°F = 43.3°C = for summer launch) T(h) is temperature at the given altitude (make sure to convert to K!) g = 9.8 m s⁻² = gravitational constant M = 0.0289652 kg mol⁻¹ = molar mass of air R = 8.3144 J mol⁻¹ K⁻¹ = universal gas constant

Liquid Flow Rate Calculations Typical venturi scrubber liquid to gas ratios:

- 0.4 to 1.3 L/m³ [5]
- 7 to 10 gallons per 1000 ft³, which is 0.93 to 1.3 L/m³ [5]
- 5-7 gallons per 1000 ft³, which is 0.66 to 0.93 L/m³ [5]

We are going to assume a liquid to gas ratio of 5 gallons per ACFM, which is 0.6 liters per m³.

Our rocket varies between 0 and 270 m s⁻¹. Assuming the rocket has a 1" hole, max air flow rate is 0.1368 m³ s⁻¹. That means peak liquid pump rate is 0.1368 * 0.6 = 0.08208 L s⁻¹ = 8.208 * 10⁻⁵ m³ s⁻¹ (or about 4.92 Liters per minute).

Let's understand if that's feasible from a peristaltic pump. Assume a ¼" (0.00635 meter) ID (on the peristaltic pump tube, and a peristaltic pump diameter of 1.5" (0.0381 meter). That gives the peristaltic pump a cross section of 0.00003167 m². Thus flow velocity must

be 2.59 m s^{-1} . For a radius of 0.01905 m , that means the peristaltic pump must spin 135.9 rotations per second (about $8,100 \text{ rpm}$). This is well above the max speed of a Nema 17 stepper motor and would almost certainly not work. We could solve this issue through parallel pumping. Assuming a maximum Nema 23 speed of 1000 rpm , we would need to run 8 parallel tubes. This is not terribly practical (though necessary if needed). A peristaltic pump is not suited for these high flow rates and therefore an alternative should be explored.

HiLetgo sells 12v submersible water pumps with $4\text{L}/\text{min}$ pumping capabilities ([link](#)). For $\$14$, two arrive, which allows for flow rates up to $8\text{L}/\text{min}$, which is plenty for our application. These pumps would live inside the liquid tank on the upper section of the payload.

Though submersible water pumps like the one quoted above were not used in the final design due to the extra requirements of a large pressure head to atomize the water through the nozzle, they nonetheless stood as a backup

4.5 Testing

4.5.1 Coulter Counter Lab Testing

Before the aperture tube could be handled (for measurements, test fits, etc...) it had to be safely unboxed and an environment had to be constructed where it could be operated on without risk of contamination.

Therefore, a cleanroom was constructed to house the aperture tube experiments, as well as a "clean box" which blows HEPA filtered air through the top of the box and across the experiments, ensuring no dust has a chance to settle on the aperture tube and threaten the experiment. Below are photos of both:



Figure 51: Cleanroom Work Bench

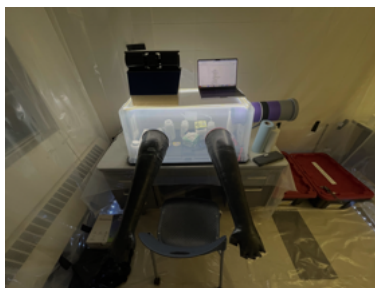


Figure 52: **Cleanbox**

In addition to constructing the rooms, procedures were also developed for setting up and operating within the clean environment. Below are itemized lists of all materials used for the testing. Exterior supplies are tools and consumables stored outside the cleanbox. Interior supplies are tools and consumable stored inside the cleanbox.

Exterior supplies

- Spare storage container
- Clean box & clean-box lid
- Large garbage bags
- Extension cable
- Nitrile exam gloves
- Speaker (for music)
- Kimtech wipes
- IPA
- Sharpie
- Printer paper
- Masking tape

Interior tools

- Plastic shoe box
- 2 × beaker sets ([link](#))
- Digital scale ([link](#))
- 1-L polypropylene bottle ([link](#))

- Clean-room notepad ([link](#))
- Ball-point pens
- Glass stir rod ([link](#))
- Wire snips
- 2 × spray bottles (body & lid)
- Multimeter
- Scissors
- Micropipette

Interior consumables

- Plastic shoe box
- 2 × clean-room wipes ([link](#))
- Baggies ([link](#))
- 2 × isopropyl alcohol
- 4 × DI water ([McMaster](#))
- NaCl crystals ([link](#))
- Parafilm ([link](#))
- Weigh boats ([link](#))
- 1-inch Kapton tape
- Micropipette tips

4.5.2 Procedure

1. **Prior to set-up** Label all containers, beakers, and spray bottles.
2. **Set up clean box**
 - 2.a) Set up folding table.
 - 2.b) Place clean box (with sealed lid) on top.
 - 2.c) Run extension cable from nearest outlet to table.
 - 2.d) Place empty storage container next to clean box containing:
 - Kimtech wipes

- Spare IPA bottles
 - Spare DI bottles
 - Spare clean-room wipes
 - Spare micropipette tips
 - Spare baggies
 - Spare weigh boats
 - Large garbage bags
 - Printer paper
3. **Load interior materials** Lift the clean-box body and place the “Interior tools” and “Interior consumables” inventories inside (see lists above).
 4. Turn on the clean-box fan.
 5. **Clean**
 - 5.a) Set up garbage bag, clean-room wipes, and a 1000-mL waste beaker.
 - 5.b) *IPA bottle rinse*: repeat three times (add ~25 mL IPA, shake, dump to waste).
 - 5.c) Fill IPA bottle half-full.
 - 5.d) *Water bottle rinse*: repeat three times (add ~25 mL water, shake, dump to waste).
 - 5.e) Fill water bottle half-full.
 - 5.f) Wipe all interior surfaces, then wipe every interior tool.
 - 5.g) Dispose of wipes in the garbage bag.
 6. **Prepare aperture-tube bottle**
 - 6.a) Rinse the PP bottle three times with ~25 mL DI water (shake & dump).
 - 6.b) Fill the PP bottle with ~100 mL DI water.
 7. **Cleanup**
 - 7.a) Cover the clean box and storage box with garbage bags.
 - 7.b) Leave a note indicating completion and readiness for the next test.

4.5.3 Test 1: Measure Resistance

Goal Empirically observe the resistance of salt water across the aperture.

Required Materials

- All interior tools & consumables from Test 0
- Aperture tube
- 316 SS wire ([McMaster](#))
- 0.1 μm liquid filters ([link](#))
- 100-mL Luer-lock syringes ([link](#))

Procedure

1. Transfer materials

- 1.a) Move the aperture tube and 316 SS wire into the clean box.
- 1.b) Store the aperture tube inside the PP bottle and remove external packaging.

2. Setup

- 2.a) Tare a 100-mL beaker on the scale; add ~ 50 g DI water and record the exact mass.
- 2.b) Prepare two electrodes: cut two 6-inch wire sections and coil one of them.

3. Experiment (8 iterations)

- 3.1. Measure the resistance between electrodes; record the value.
- 3.2. Empty any liquid from the aperture tube back into the beaker.
- 3.3. Weigh 0.25 g NaCl, recording the exact mass; add it to the water and stir until dissolved.
- 3.4. Fill the aperture tube with the saline solution using the micropipette.
- 3.5. Insert the straight electrode into the aperture tube; place the coiled electrode in the beaker.

4. Cleanup

- 4.a) Rinse the aperture tube and electrodes with DI water; dry and bag them.
- 4.b) Dispose of salt solution and wipe all glassware with DI water and IPA.
- 4.c) Remove the garbage bag, turn off the clean box, and bag the clean-box exterior and storage box.

4.5.4 Test 2: Observe Voltage Spikes

Goal Detect voltage spikes caused by dust particles transiting through the aperture tube.

Required Materials

- Interior tools & consumables
- Aperture tube & electrodes
- 150–500nm aluminum dust ([link](#))
- Vacuum pump
- Oscilloscope

Procedure (Abbreviated)

1. Dust prep outside the clean box

- 1.a) Weigh ~ 0.1 g dust onto a weigh boat, record mass, transfer to a second boat, and measure residue on the first.
- 1.b) Repeat for a second aliquot; seal both in a baggie.
- 1.c) Wipe the scale with IPA and Kimwipes.

2. Transfer and clean

- 2.a) Load the oscilloscope, scale, and sealed dust boat into the clean box.
- 2.b) Turn on the clean-box fan and wipe all items and interior surfaces with IPA.

3. Salt-water baseline

- 3.a) Prepare 50g DI water in a beaker, record mass, add measured NaCl, mix, and fill the aperture tube with the saline.
- 3.b) Submerge the aperture tip into the beaker; insert the straight electrode into the tube and the coiled electrode into the beaker.

4. Experiment

- 4.a) (Steps for dust injection, vacuum draw, and oscilloscope monitoring go here.)

Below is a photograph of the flow testing



Figure 53: Picture of the Aperture Tube Testing



Figure 54: Picture of the Testing Setup in the ELL

4.5.5 Resistance vs Salinity

Pure water is not very conductive, which makes measuring small changes in resistance challenging. Therefore, an electrolyte is typically introduced into coulter counters. In the case of the rocketry payload, ultra-pure NaCl was used due to its wide availability and well-established use in literature.

However, the concentration of NaCl has a significant, nonlinear effect on conductivity. While there are established NaCl concentration vs conductivity relationships, the small and unknown topology of the aperture tube makes it nearly impossible to use those relationships to predict resistance of the aperture tube from theory alone.

Therefore, several measurements were taken by incrementally adding known amounts of NaCl to a known amount of water and measuring the corresponding resistance. Below is a plot of the experimentally observed results, along with a quadratic best fit.

Incremental NaCl Mass	Observed Voltage	Total NaCl mass	Salt mass/water mass	Derived resistance (Ω)
0	9.98	0	0.00000	7494980
0.57	8.77	0.57	0.01075	107094
0.55	8.14	1.12	0.02112	65733
0.6	7.57	1.72	0.03244	46791
0.54	7.29	2.26	0.04263	40404
0.63	6.89	2.89	0.05451	33276
0.56	6.59	3.45	0.06907	29027
0.64	6.37	4.09	0.07714	26357
0.61	5.99	4.7	0.08965	22436
0.59	5.79	5.29	0.09977	20657
1.03	5.405	6.32	0.11620	17968
1.04	5.17	7.36	0.13882	16077
1.83	4.8	9.19	0.17333	13865

Figure 55: Table Containing Experimentally Measured Resistances of the 20 m Beckman Coulter Aperture Tube

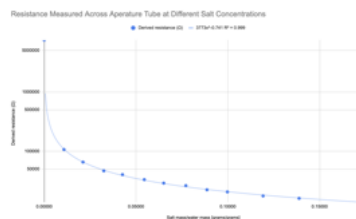


Figure 56: Graph of Experimentally Measured Aperture Tube Resistances

4.6 Manufacturing

A majority of payload components were 3D printed, owing to the rapid turn around and ability to easily create complex geometries.

Final parts were 3D printed out of clear PETG, which allows for some visibility into the inside of the part which is helpful for diagnosing issues with the fluid system, as well as contributing to the overall aesthetic of the payload.

There were six distinct machine components

- 1x Tip
- 1x Tip nut
- 1x Superstructure top plate
- 4x Superstructure vertical posts
- 1x Superstructure bottom plate
- 1x Superstructure bulkhead

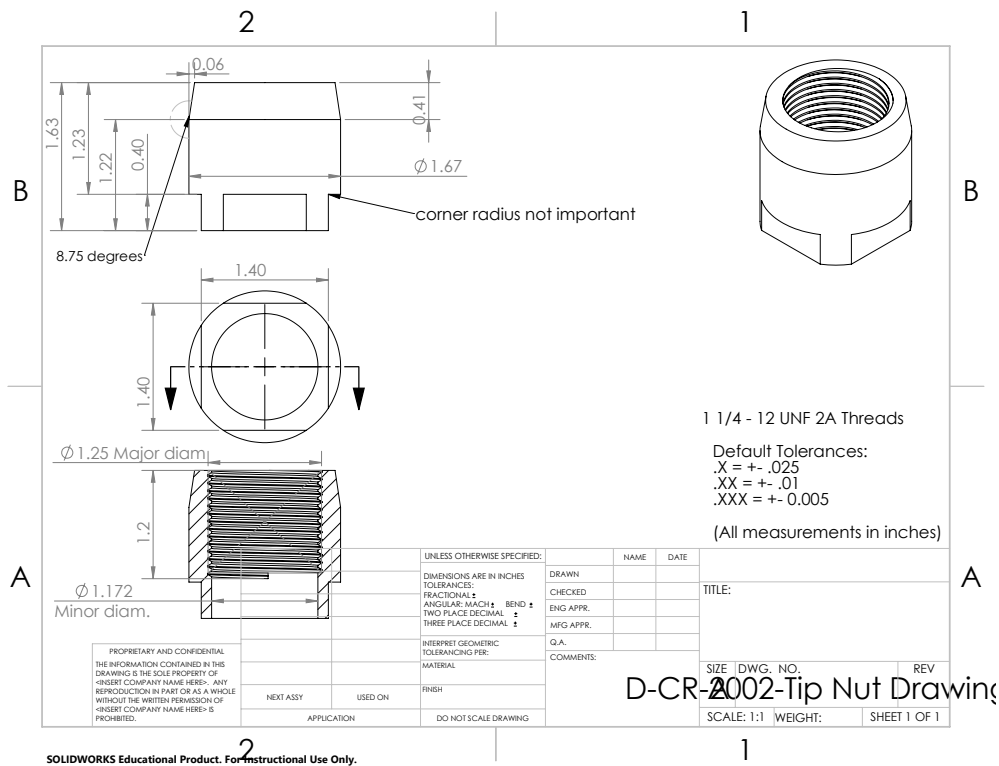
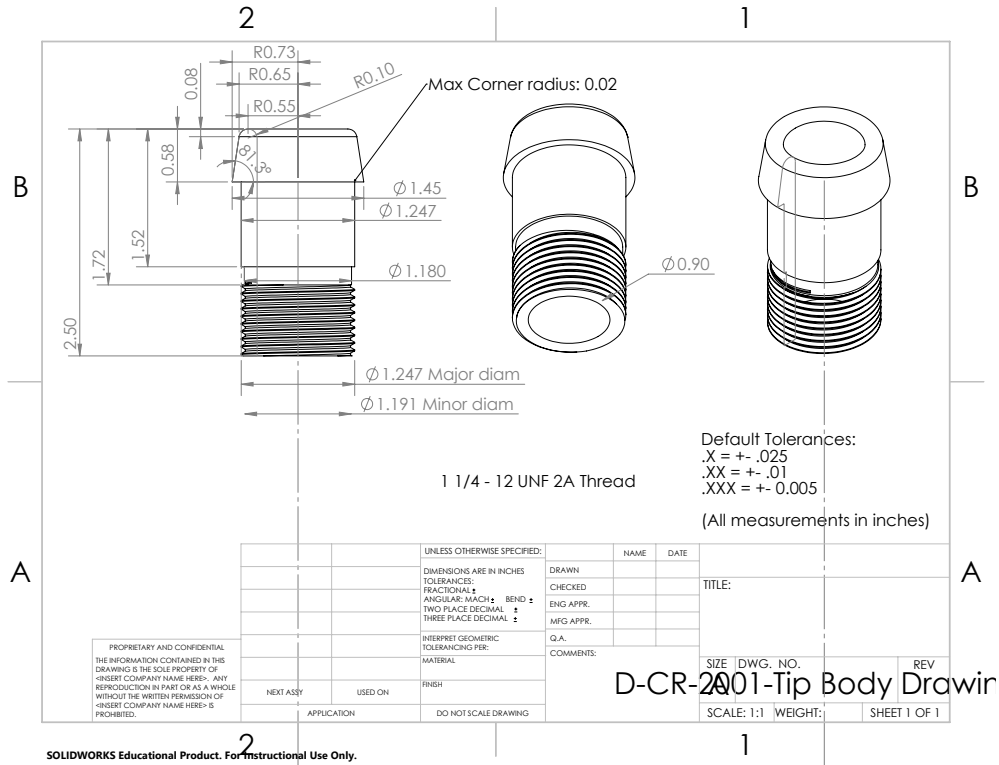
Each vertical post was an identical part, reducing complexity of manufacturing. When assembled, the posts were rotated in a specific manor to ensure holes were positioned in the correct location.

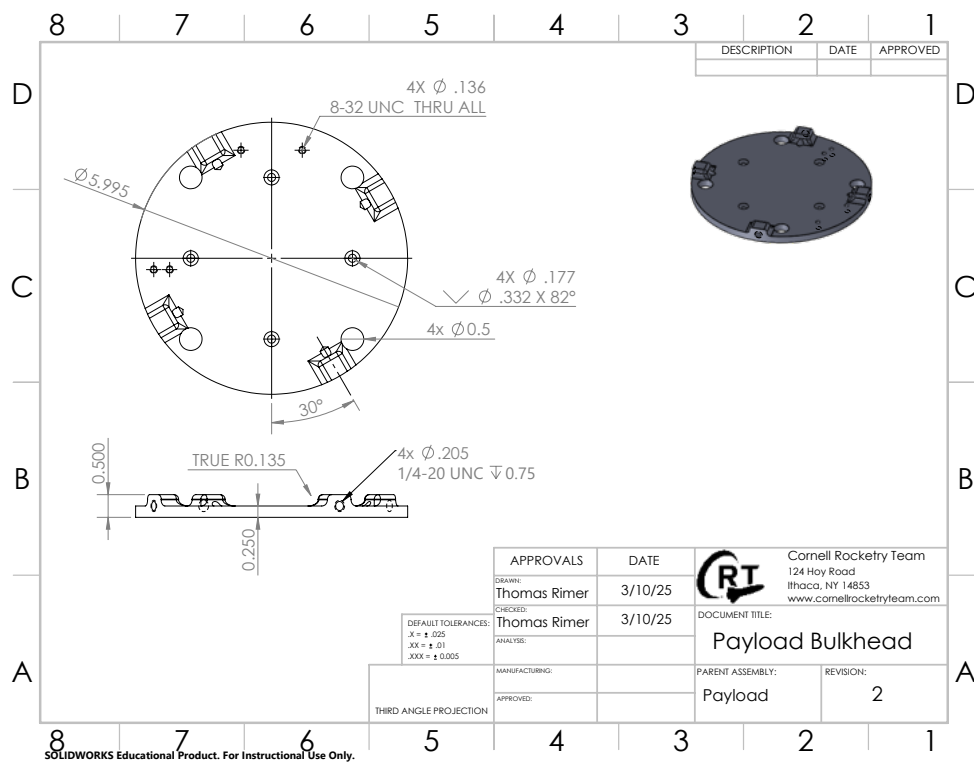
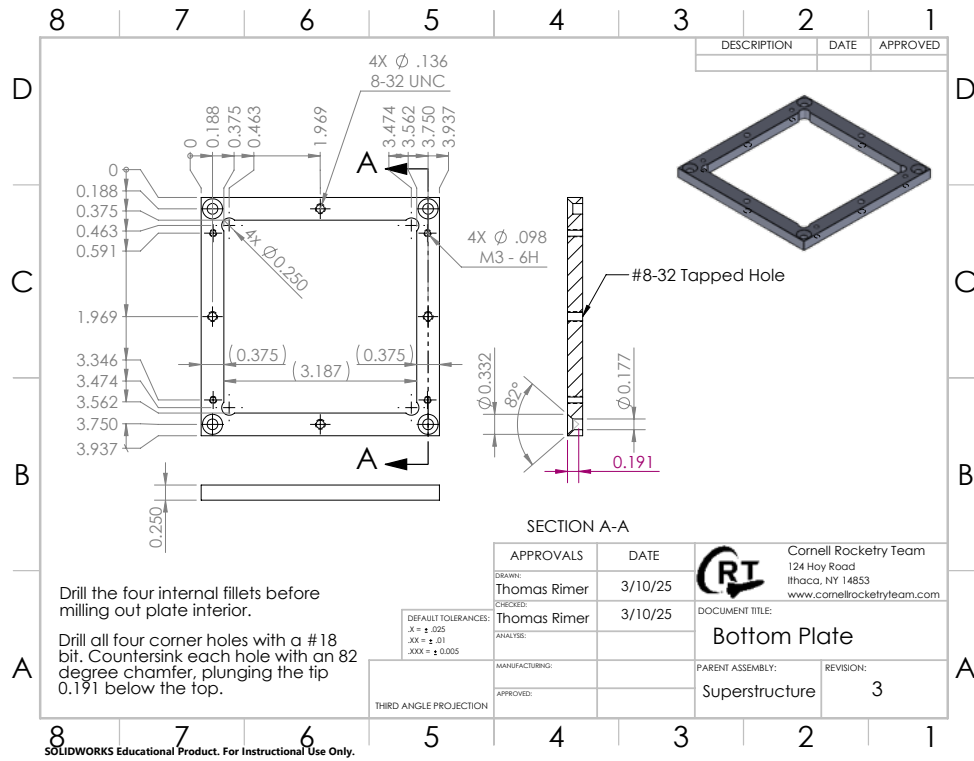
4.7 Supply Chain

Most components within the payload were either CNC machined or 3D printed by rocketry members, which makes payload relatively insulated from supply chain issues. The singular major exception is the 20 m aperture tube, which Beckman Coulter does not offer as a commercial product. To obtain it, I reached out directly to their product engineers and explain our project and they sent us one.

4.8 Appendix

Below are the machinists' drawings for the six different machined components





References

- [1] International Rocket Engineering Competition Rules and Requirements Document
https://www.soundingrocket.org/uploads/9/0/6/4/9064598/irec_rules_and_requirements_document_v_1.6_.pdf
- [2] Featherweight GPS Tracker
<https://www.featherweightaltimeters.com/featherweight-gps-tracker.html>
- [3] Beckman Coulter Aperture Tubes
<https://www.beckman.com/supplies/aperture-tube>
- [4] Seymour Calvert. *Venturi and Other Atomizing Scrubbers Efficiency and Pressure Drop*. AIChE Journal, 1970.
- [5] Daniel Mussatti, Paula Hemmer. *Wet Scrubbers for Particulate Matter*. EPA, 2002.
- [6] White Sands as a Dust Emission Hotspot
<https://www.nps.gov/articles/white-sands-as-dust-emission-hotspot.htm>